Theory of interparticle correlations in dense, high-temperature plasmas. III. Thermodynamic functions

Shigenori Tanaka, Shinichi Mitake, Xin-Zhong Yan, and Setsuo Ichimaru
Department of Physics, University of Tokyo, Bunkyo-ku, Tokyo 113, Japan
(Received 10 December 1984)

On the basis of the general formalism and the analysis of the correlation functions presented in the preceding two papers (I and II), we calculate in this paper (III) various thermodynamic functions with explicit inclusion of the varied degrees of the electron degeneracy and the local-field corrections describing the strong Coulomb-coupling effects. The physical implications of the computed results are investigated through comparison with other model calculations. Mindful of practical applications of the present theory, we derive the analytic interpolation formulas parametrizing the computed results accurately for the thermodynamic functions.

I. INTRODUCTION

In the first paper in this series,[1] referred to as paper I, we presented a general formalism for the analysis of interparticle correlations in dense, high-temperature plasmas. The formalism was applied to explicit calculation and investigation of correlation functions in the preceding paper,[2] referred to as paper II. In the present paper (paper III in the series), we calculate various thermodynamic functions, investigate their physical implications through comparison with other model calculations, and derive the analytic interpolation formulas which may be of use in practical applications.

For definiteness in the numerical analysis, we confine ourselves to consideration of two-component hydrogenic plasmas, where $Z=1$. The parameter domain of interest has been specified in connection with Fig. 1 in paper I, whose notation we follow here unless otherwise specified.

The thermodynamic properties of dense plasmas have been considered by various investigators[3–7] in the past. Except for the molecular-dynamics simulation work of Hansen and McDonald,[6] where the plasma is modeled as a classical system of interacting pseudoparticles, those authors treated parameter domains where it was not necessary to take account of varied degrees of the electron degeneracy[8,9] or the local-field corrections[8–10] (LFC's) describing the correlation effects beyond the random-phase approximation (RPA). The present paper aims at elucidating the effects of both the electron degeneracy and the LFC's on the thermodynamic functions through a formalism with a reliable accuracy.

II. INTERACTION ENERGY

In paper II (Ref. 2) we have evaluated the static-structure factors $S_{11}(k)$, $S_{22}(k)$, and $S_{12}(k)$ for combinations of the electron-degeneracy parameter $\theta=0.1$, 1, and 10 and the Coulomb-coupling constant $\Gamma\leq 2$. With the knowledge of those static-structure factors, the interaction energy $E_{\rm int}$ of the hydrogen plasma is calculated as[1,10]

$$E_{\rm int}=E_{11}+E_{22}+E_{12}\ , \tag{1}$$

$$\frac{E_{11}}{Nk_BT}=\frac{1}{4\pi^2k_BT}\int d\mathbf{k}\frac{e^2}{k^2}[S_{11}(k)-1]\ , \tag{2a}$$

$$\frac{E_{22}}{Nk_BT}=\frac{1}{4\pi^2k_BT}\int d\mathbf{k}\frac{e^2}{k^2}[S_{22}(k)-1]\ , \tag{2b}$$

$$\frac{E_{12}}{Nk_BT}=\frac{-2}{4\pi^2k_BT}\int d\mathbf{k}\frac{e^2}{k^2}S_{12}(k)\ . \tag{2c}$$

Here N refers to the total number of the electrons or the ions, $E_{\mu\nu}$ $(\mu,\nu=1,2)$ denotes the partial contribution to the total interaction energy arising from correlations between the μ- and ν-species particles.

In Tables I–III we list the numerical results of the computations with and without inclusion of the LFC's for 32 parametric combinations of θ and Γ. Since Γ, θ, and the electron-density parameter r_s are related via

$$\Gamma\theta=2(4/9\pi)^{2/3}r_s\ , \tag{3}$$

a large Γ implies strong Coulomb coupling, not only in the ion system, but also in the electron system at a relatively high temperature $\theta\gtrsim 0.1$, for instance. The computed results in those tables show that the Coulomb-coupling effects represented by the LFC's become significant even at a relatively modest value of $\Gamma\simeq 1$.

It is instructive to note the behaviors of E_{11}/Nk_BT and E_{22}/Nk_BT in the small-Γ domain. While the ionic interaction energy behaves according to the Debye-Hückel prediction $\sim\Gamma^{3/2}$, the electronic counterpart varies proportionally to Γ; the latter shows dominance of the Hartree-Fock (HF) exchange energy. Owing to these different behaviors, a crossover in the relative magnitude between E_{11}/Nk_BT and E_{22}/Nk_BT takes place at a certain Γ value; with LFC this Γ value is observed in the vicinity of 0.5 and in RPA it takes on a somewhat reduced value.

The onset of ion-electron decoupling brought about by the electron degeneracy is apparent in Tables I–III. At $\theta=10$, the electrons may be regarded as classical particles; the interaction energy between ions and electrons takes on a magnitude greater than the interionic or interelectronic energies ($|E_{12}|>|E_{11}|\simeq|E_{22}|$). At $\theta=0.1$, on the other hand, the electrons are almost completely degenerate

TABLE I. Partial contributions to the total interaction energy at $\theta=0.1$ obtained from Eqs. (2). LFC and RPA refer to the computations with and without inclusion of LFC's, respectively.

	$-E_{11}/Nk_BT$		$-E_{22}/Nk_BT$		$-E_{12}/Nk_BT$	
Γ	LFC	RPA	LFC	RPA	LFC	RPA
0.03	1.3212×10^{-2}	1.3213×10^{-2}	4.1208×10^{-3}	4.1993×10^{-3}	1.1705×10^{-3}	1.1692×10^{-3}
0.05	2.2072×10^{-2}	2.2077×10^{-2}	8.7419×10^{-3}	9.0363×10^{-3}	2.4741×10^{-3}	2.4685×10^{-3}
0.1	4.4336×10^{-2}	4.4373×10^{-2}	2.3877×10^{-2}	2.5565×10^{-2}	6.7859×10^{-3}	6.7446×10^{-3}
0.2	8.9201×10^{-2}	8.9427×10^{-2}	6.3411×10^{-2}	7.2345×10^{-2}	1.8468×10^{-2}	1.8177×10^{-2}
0.3	1.3437×10^{-1}	1.3500×10^{-1}	1.1030×10^{-1}	1.3297×10^{-1}	3.3079×10^{-2}	3.2197×10^{-2}
0.5	2.2528×10^{-1}	2.2750×10^{-1}	2.1654×10^{-1}	2.8637×10^{-1}	6.8904×10^{-2}	6.5454×10^{-2}
0.7	3.1662×10^{-1}	3.2162×10^{-1}	3.3252×10^{-1}	4.7480×10^{-1}	1.1193×10^{-1}	1.0365×10^{-1}
1	4.5387×10^{-1}	4.6553×10^{-1}	5.1668×10^{-1}	8.1171×10^{-1}	1.8799×10^{-1}	1.6744×10^{-1}
2	9.0861×10^{-1}	9.6573×10^{-1}	1.1638	2.3042	5.2971×10^{-1}	4.1470×10^{-1}

and the ion-electron coupling is much depressed.

The observation mentioned above offers another justification for the use of Eq. (I.36) or Eq. (I.44c) [in paper I (Ref. 1)] in the present dense-plasma problem. As we have remarked in connection with Fig. 1 in paper I, the regime A ($\theta\geq10$) coincides with that of weak-Coulomb coupling ($\Gamma\leq0.1$); here the RPA gives an accurate description of the correlation effects. Hence we may legitimately use Eq. (I.36), although $|E_{12}|$ may be larger than $|E_{11}|$ and $|E_{22}|$. As the value of θ decreases, the electron degeneracy acts to lessen the effects of $G_{12}(k)$ and $G_{21}(k)$; Eq. (I.44c) may thus be used with a good accuracy.

III. FREE ENERGY

The Helmholtz free energy of the system is

$$F=F_0+F_{\rm ex}\ , \tag{4}$$

where F_0 is a sum of the free energies of the ideal-gas electron system and the ideal-gas ion system. The excess free energy $F_{\rm ex}$ is calculated according to[10]

$$f_{\rm ex}(\Gamma,\theta)\equiv\frac{F_{\rm ex}}{Nk_BT}=\frac{F_{\rm ex}(\Gamma_0)}{Nk_BT}\bigg|_\theta+\int_{\Gamma_0}^{\Gamma}d\Gamma\frac{1}{\Gamma}\frac{E_{\rm int}}{Nk_BT}\bigg|_\theta\ , \tag{5}$$

where $|_\theta$ means that θ be kept constant. As in Eq. (1), the excess free energy per ion-electron pair $f_{\rm ex}$ is likewise expressed as a sum of the partial contributions:

$$f_{\rm ex}=f_{11}+f_{22}+f_{12}\ . \tag{6}$$

The two-component Debye-Hückel (TCDH) theory predicts that $f_{11}=f_{22}=-\Gamma^{3/2}/\sqrt{6}$ and $f_{12}=-(2/\sqrt{6})\Gamma^{3/2}$.

Figures 1–4 exhibit the excess free energies at $\theta=1$ calculated according to Eq. (5) where the values of the interaction energies listed in Table II are used. Since the integration from $\Gamma_0=0$ to any Γ in Eq. (5) can be explicitly carried out in the RPA scheme, we have evaluated the integrations pertaining to the free energies in the LFC scheme by Simpson's method, choosing the smallest Γ value for each θ as Γ_0 and the corresponding RPA value as $F_{\rm ex}(\Gamma_0)$.

Figure 1 shows the contribution of the electron-electron interaction f_{11} divided by Γ. In the limit of $\Gamma\to0$, both the LFC and RPA values approach the HF value,[8,11]

$$\frac{F_1}{Nk_BT}=-\frac{1}{nk_BT}\int\frac{d\mathbf{k}}{(2\pi)^3}\int\frac{d\mathbf{q}}{(2\pi)^3}\frac{4\pi e^2}{|\mathbf{k}-\mathbf{q}|^2}\times f_0(k)f_0(q)\ . \tag{7}$$

Here $f_0(k)$ is the Fermi distribution

TABLE II. The same as Table I at $\theta=1$.

	$-E_{11}/Nk_BT$		$-E_{22}/Nk_BT$		$-E_{12}/Nk_BT$	
Γ	LFC	RPA	LFC	RPA	LFC	RPA
0.01	2.1220×10^{-3}	2.1230×10^{-3}	6.4243×10^{-4}	6.4699×10^{-4}	9.8272×10^{-4}	9.8237×10^{-4}
0.03	7.1118×10^{-3}	7.1308×10^{-3}	3.2854×10^{-3}	3.3635×10^{-3}	4.9591×10^{-3}	4.9498×10^{-3}
0.05	1.2626×10^{-2}	1.2700×10^{-2}	6.9479×10^{-3}	7.2413×10^{-3}	1.0474×10^{-2}	1.0432×10^{-2}
0.1	2.7730×10^{-2}	2.8178×10^{-2}	1.8823×10^{-2}	2.0510×10^{-2}	2.8742×10^{-2}	2.8434×10^{-2}
0.2	6.0809×10^{-2}	6.3362×10^{-2}	4.9178×10^{-2}	5.8157×10^{-2}	7.8655×10^{-2}	7.6479×10^{-2}
0.3	9.5384×10^{-2}	1.0225×10^{-1}	8.4157×10^{-2}	1.0709×10^{-1}	1.4203×10^{-1}	1.3539×10^{-1}
0.4	1.3008×10^{-1}	1.4378×10^{-1}	1.2144×10^{-1}	1.6523×10^{-1}	2.1670×10^{-1}	2.0223×10^{-1}
0.5	1.6409×10^{-1}	1.8738×10^{-1}	1.5981×10^{-1}	2.3138×10^{-1}	3.0167×10^{-1}	2.7538×10^{-1}
0.6	1.9686×10^{-1}	2.3269×10^{-1}	1.9847×10^{-1}	3.0475×10^{-1}	3.9644×10^{-1}	3.5378×10^{-1}
0.7	2.2792×10^{-1}	2.7946×10^{-1}	2.3690×10^{-1}	3.8473×10^{-1}	5.0077×10^{-1}	4.3670×10^{-1}
0.8	2.5691×10^{-1}	3.2750×10^{-1}	2.7466×10^{-1}	4.7088×10^{-1}	6.1458×10^{-1}	5.2356×10^{-1}
0.9	2.8351×10^{-1}	3.7667×10^{-1}	3.1141×10^{-1}	5.6282×10^{-1}	7.3788×10^{-1}	6.1393×10^{-1}
1	3.0743×10^{-1}	4.2686×10^{-1}	3.4686×10^{-1}	6.6026×10^{-1}	8.7080×10^{-1}	7.0747×10^{-1}

TABLE III. The same as Table I at $\theta=10$.

Γ	$-E_{11}/Nk_BT$ LFC	$-E_{11}/Nk_BT$ RPA	$-E_{22}/Nk_BT$ LFC	$-E_{22}/Nk_BT$ RPA	$-E_{12}/Nk_BT$ LFC	$-E_{12}/Nk_BT$ RPA
0.003	1.5609×10^{-4}	1.5616×10^{-4}	1.0054×10^{-4}	1.0148×10^{-4}	1.9796×10^{-4}	1.9795×10^{-4}
0.005	3.0669×10^{-4}	3.0698×10^{-4}	2.1616×10^{-4}	2.1732×10^{-4}	4.2504×10^{-4}	4.2498×10^{-4}
0.01	7.8141×10^{-4}	7.8347×10^{-4}	6.0920×10^{-4}	6.1375×10^{-4}	1.1965×10^{-3}	1.1960×10^{-3}
0.03	3.5471×10^{-3}	3.5898×10^{-3}	3.1112×10^{-3}	3.1891×10^{-3}	6.1491×10^{-3}	6.1368×10^{-3}
0.05	7.1941×10^{-3}	7.3632×10^{-3}	6.5700×10^{-3}	6.8627×10^{-3}	1.3147×10^{-2}	1.3091×10^{-2}
0.07	1.1433×10^{-2}	1.1845×10^{-2}	1.0680×10^{-2}	1.1370×10^{-2}	2.1685×10^{-2}	2.1536×10^{-2}
0.1	1.8587×10^{-2}	1.9630×10^{-2}	1.7735×10^{-2}	1.9417×10^{-2}	3.6875×10^{-2}	3.6455×10^{-2}
0.2	4.6441×10^{-2}	5.2424×10^{-2}	4.6011×10^{-2}	5.4950×10^{-2}	1.0394×10^{-1}	1.0091×10^{-1}
0.5	1.3744×10^{-1}	1.9087×10^{-1}	1.4640×10^{-1}	2.1755×10^{-1}	4.2070×10^{-1}	3.8270×10^{-1}
1	2.4459×10^{-1}	5.0141×10^{-1}	3.0455×10^{-1}	6.1681×10^{-1}	1.2773	1.0153

$$f_0(k)=\frac{1}{\exp[(\epsilon_k-\mu_0)/k_BT]+1} \tag{8}$$

with $\epsilon_k=\hbar^2k^2/2m$, where the Fermi level μ_0 is determined from the normalization condition

$$\frac{n}{2}=\int_0^\infty dk\frac{k^2}{2\pi^2}f_0(k)\ . \tag{9}$$

Numerical values pertaining to the integrals in Eqs. (7) and (9) are tabulated in the Appendix. We find in Fig. 1 that the TCDH model deviates widely from the present result (LFC or RPA) because it fails to account for the exchange effect.

The contribution to the free energy of the electron gas, stemming from the summation of the ring diagrams, is given by[8,11]

$$\frac{F_r}{Nk_BT}=\frac{3}{4}\sum_{l=-\infty}^{\infty}\int_0^\infty dy\,y^2\{\ln[1+\Psi_l(y)]-\Psi_l(y)\}\ , \tag{10}$$

where

$$\Psi_l(y)=\left[\frac{9\pi}{4}\right]^{1/3}\frac{\Gamma\theta}{\pi y^3}\times\int_0^\infty dx\,xf_0(k_Fx)\times\ln\left[\frac{(2\pi l\theta)^2+(y^2+2xy)^2}{(2\pi l\theta)^2+(y^2-2xy)^2}\right], \tag{11}$$

and $k_F=(3\pi^2n)^{1/3}$. The sum of Eqs. (7) and (10) is also plotted in Fig. 1 as HF + RING. The difference between this evaluation and the RPA result reflects the influence of the ion system upon the electron-electron correlations.

The ion-ion excess free energy f_{22} divided by $\Gamma^{3/2}$ is plotted in Fig. 2. The LFC result deviates remarkably from the RPA result, indicating significant involvement of the non-RPA Coulomb-coupling effects. For comparison we have also plotted the free-energy values in the one-component Debye-Hückel (OCDH) model and those obtained by Brami, Hansen, and Joly[12] (BHJ) for the one-component plasma (OCP) in the hypernetted-chain approximation. It is noteworthy that the relation between

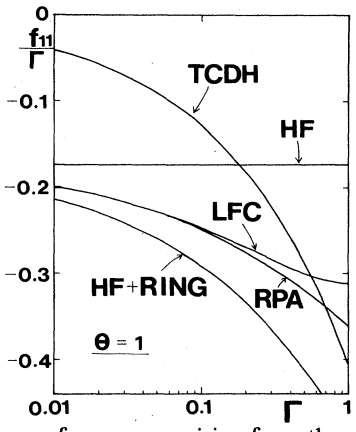

FIG. 1. Excess free energy arising from the electron-electron interaction f_{11} divided by Γ at $\theta=1$ in various models. LFC and RPA refer to the calculations with and without inclusion of the local-field corrections, respectively; TCDH, the two-component Debye-Hückel theory; HF, the Hartree-Fock approximation; RING, the contribution from the sum of the ring diagrams.

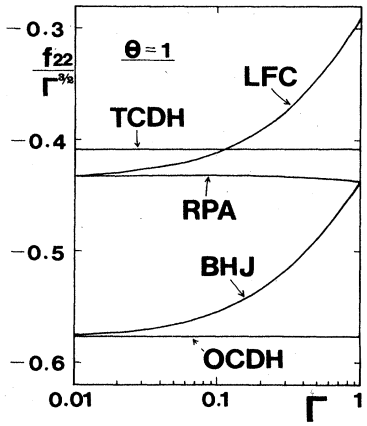

FIG. 2. Excess free energy arising from the ion-ion interaction f_{22} divided by $\Gamma^{3/2}$ at $\theta=1$ in various models. OCDH refers to the calculations based on the one-component Debye-Hückel theory; BHJ, the analytic expression given by Brami, Hansen, and Joly (Ref. 11); LFC and RPA have the same meaning as those in Fig. 1.

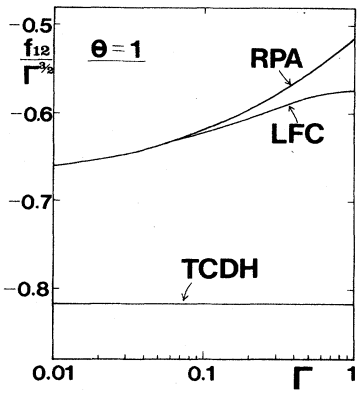

FIG. 3. Excess free energy arising from the electron-ion interaction f_{12} divided by $\Gamma^{3/2}$ at $\theta=1$ in various models. See Fig. 1 for the meaning of LFC, RPA, and TCDH.

the LFC and RPA curves is quite analogous to that between the BHJ and OCDH curves, as we would have expected. As Γ increases, f_{22} tends to be proportional to Γ due to the strong Coulomb-coupling effects;[10] we observe this behavior in the LFC and BHJ curves. The departure of the RPA curve from the TCDH curve reflects the effects of electron degeneracy.

As we note from the comparison between the magnitudes of the RPA and TCDH values in Fig. 3, the electron degeneracy acts to lessen the electron-ion coupling. The discrepancy decreases as the temperature is raised to $\theta=10$.

We show the total excess free energy f_{ex} divided by $\Gamma^{3/2}$ in Fig. 4. In spite of a considerable departure observed in the computed results of each partial contribution, the LFC and RPA values for f_{ex} differ only slightly. This is because the LFC's tend to decrease the magnitudes of f_{11} and f_{22}, and increase that of f_{12}; the effects of the LFC's are thus partially compensated. For small Γ, the electron-electron exchange contribution is dominant; the TCDH model is inadequate even at a small Γ. The HF + RING + BHJ curve represents a simple sum of the partial contributions of the two OCP's. This model underestimates the magnitude of the total excess free energy by about (10—25)% as compared with the LFC result.

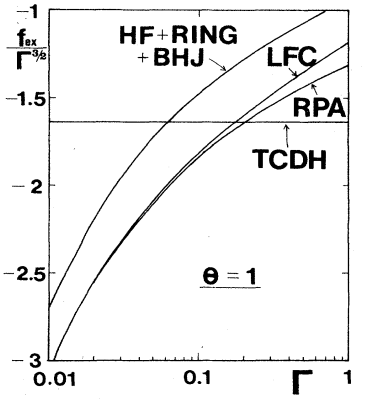

FIG. 4. Total excess free energy f_{ex} divided by $\Gamma^{3/2}$ at $\theta=1$ in various models. See Figs. 1 and 2 for the meaning of the abbreviated symbols.

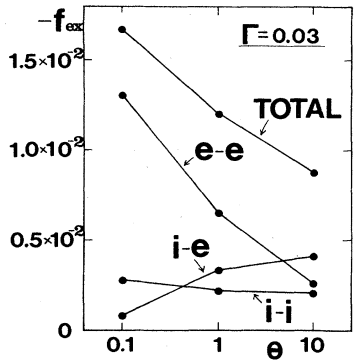

FIG. 5. Absolute value of the excess free energy $-f_{ex}$ at $\Gamma=0.03$ for $\theta=0.1$, 1, and 10 based on the calculations with inclusion of the LFC's; the lines connecting them are only to guide the eye. *e-e*, *i-i*, and *i-e* refer to the partial contributions arising from the electron-electron, the ion-ion, and the ion-electron interactions, respectively; TOTAL, the sum of those three contributions.

The dependence of the total excess free energy upon the degree of the electron degeneracy is not simple. Figures 5 and 6 illustrate the θ dependence of $-f_{ex}$ at $\Gamma=0.03$ and 1 evaluated in the LFC scheme. Since Γ is fixed, the ion-ion contribution remains almost constant regardless of θ. The magnitude of the electron-electron contribution decreases gradually as θ increases owing to reduction in the exchange energy. At $\Gamma=1$, however, this tendency is not so remarkable as at $\Gamma=0.03$ since the Coulomb correlations act to compensate this reduction. The magnitude of the ion-electron excess free energy, on the contrary, increases with θ because of the change in the degree of electron degeneracy. The total excess free energy is determined on the balance between those factors.

IV. EQUATION OF STATE

In order to derive the equation of state for the dense, high-temperature plasma out of the numerical data tabulated in Tables I—III, we must find an analytic formula parametrizing those data which is sufficiently accurate to enable the necessary integration and differentiation.

The fitting formula for the total interaction energy calculated with inclusion of the LFC effect is expressed as ($\Gamma\leq2$, $\theta\geq0.1$)

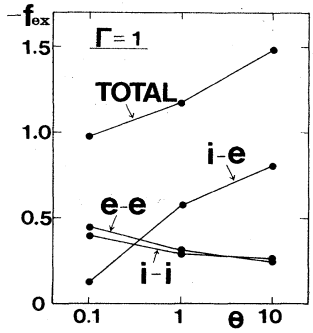

FIG. 6. Absolute value of the excess free energy $-f_{ex}$ at $\Gamma=1$ for $\theta=0.1$, 1, and 10; otherwise the same as in Fig. 5.

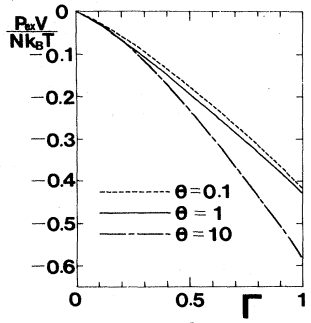

FIG. 7. Excess pressure $P_{ex}V/Nk_BT$ at $\theta=0.1$, 1, and 10 obtained from the computations with inclusion of the LFC's.

$$\frac{E_{int}}{Nk_BT}=a(\theta)\Gamma+b(\theta)\Gamma^{3/2}+c(\theta)\Gamma^2 , \tag{12}$$

where

$$a(\theta)=0.449\,73\exp(-0.547\,12/\theta)-0.443\,35 ,$$
$$b(\theta)=-1.502\,03\exp(-0.473\,57/\theta)-1.047\,75 , \tag{13}$$
$$c(\theta)=0.481\,62\exp(-0.160\,00/\theta)+0.236\,24 .$$

This formula reproduces all the computed values of E_{int} for the 32 cases with relative errors less than 2%.

The total excess free energy is then obtained by performing the Γ integration in Eq. (5) from 0 to Γ as ($\Gamma\leq 2$, $\theta\geq 0.1$)

$$f_{ex}(\Gamma,\theta)=a(\theta)\Gamma+\tfrac{2}{3}b(\theta)\Gamma^{3/2}+\tfrac{1}{2}c(\theta)\Gamma^2 . \tag{14}$$

This expression again reproduces the values obtained by Simpson's method in Sec. III with relative errors less than 2%.

Finally we calculate the excess pressure from Eqs. (12)—(14) as ($\Gamma\leq 2$, $\theta\geq 0.1$)

$$\begin{aligned}\frac{P_{ex}V}{Nk_BT}&=-V\left[\frac{\partial f_{ex}}{\partial V}\right]_{T,N}\\&=\frac{\Gamma}{3}\left[\frac{\partial f_{ex}}{\partial\Gamma}\right]_{\theta}-\frac{2\theta}{3}\left[\frac{\partial f_{ex}}{\partial\theta}\right]_{\Gamma}\\&=\frac{1}{3}\frac{E_{int}}{Nk_BT}+\frac{1}{\theta}[p(\theta)\Gamma+q(\theta)\Gamma^{3/2}+r(\theta)\Gamma^2] ,\end{aligned} \tag{15}$$

where V is the volume of the system, and

$$p(\theta)=-0.164\,04\exp(-0.547\,12/\theta) ,$$
$$q(\theta)=0.316\,14\exp(-0.473\,57/\theta) , \tag{16}$$
$$r(\theta)=-0.025\,686\exp(-0.160\,00/\theta) .$$

The excess pressures at $\theta=0.1$, 1, and 10 computed from Eqs. (12), (13), (15), and (16) are plotted in Fig. 7.

The total pressure of the system is computed by adding to this excess pressure the contributions arising from the noninteracting parts; the latter for the ions is nk_BT and that for the electrons is tabulated in the Appendix. The excess-pressure contribution, Eq. (15), of the interparticle correlations acts to reduce the total pressure by (8—30)% at $\Gamma=1$ for $0.1\leq\theta\leq 10$.

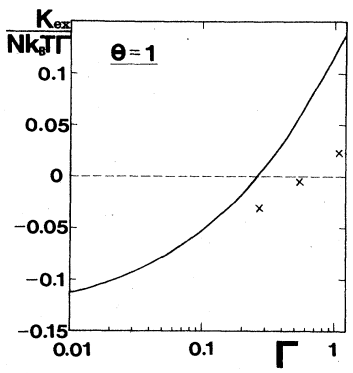

FIG. 8. Excess kinetic energy K_{ex}/Nk_BT divided by Γ at $\theta=1$ obtained from the computations with inclusion of the LFC's. Crosses represent the results for the electron OCP calculated by Pokrant (Ref. 14).

The virial theorem for the Coulombic system reads[13]

$$PV=\tfrac{1}{3}E_{int}+\tfrac{2}{3}K , \tag{17}$$

where K refers to the kinetic energy. Subtracting from Eq. (17) the noninteracting part $P_0V=\frac{2}{3}K_0$, we find

$$\frac{P_{ex}V}{Nk_BT}=\frac{1}{3}\frac{E_{int}}{Nk_BT}+\frac{2}{3}\frac{K_{ex}}{Nk_BT} . \tag{18}$$

Since the excess free energy f_{ex} of the classical system ($\theta\rightarrow\infty$) is expressible as a function of Γ alone,[10,14] we naturally have $K_{ex}=0$ in this limit. If we take the limit

TABLE IV. Numerical values of the quantities defined through Eqs. (A2)—(A4).

θ	μ_0/k_BT	$I_{3/2}(\mu_0/k_BT)$	$J(\theta)$
0.01	99.9918	4.0016×10^{4}	0.9991
0.03	33.3086	2.5755×10^{3}	0.9940
0.05	19.959	7.2290×10^{2}	0.9855
0.1	9.9164	1.3161×10^{2}	0.9536
0.2	4.8229	25.772	0.8649
0.3	3.0486	10.647	0.7694
0.4	2.1009	5.9260	0.6827
0.5	1.4862	3.8528	0.6083
0.6	1.0414	2.7496	0.5457
0.7	0.696 59	2.0863	0.4932
0.8	0.416 42	1.6523	0.4489
0.9	0.181 11	1.3507	0.4113
1	−0.021 461	1.1312	0.3791
2	−1.2307	3.7010×10^{-1}	0.2090
3	−1.8815	1.9737×10^{-1}	0.1431
4	−2.3309	1.2708×10^{-1}	0.1086
5	−2.6751	9.0503×10^{-2}	0.087 39
6	−2.9542	6.8659×10^{-2}	0.073 11
7	−3.1892	5.4382×10^{-2}	0.062 81
8	−3.3921	4.4454×10^{-2}	0.055 05
9	−3.5707	3.7218×10^{-2}	0.049 00
10	−3.7302	3.1754×10^{-2}	0.044 14
30	−5.3849	6.0905×10^{-3}	0.014 78
100	−7.1922	1.0001×10^{-3}	0.004 439

of $\theta \to 0$ (complete degeneracy) at a fixed value of Γ, we may neglect the ion-electron coupling; we also have $K_{11}=K_{22}=0$ because the ion system is classical and because the leading HF contribution to K_{11} identically vanishes in the limit of $r_s \to 0$. The total excess kinetic energy K_{ex} thus vanishes in this limit. Those boundary conditions are naturally taken care of in Eq. (15). Figure 8 exhibits the excess kinetic energy K_{ex}/Nk_BT divided by Γ computed from Eqs. (15), (16), and (18) at $\theta=1$; we here observe a change of sign from negative to positive at $\Gamma \simeq 0.3$. Calculation by Pokrant[15] for the electron OCP has shown an analogous tendency, as the crosses in Fig. 8 illustrate.

V. CONCLUDING REMARKS

We have carried out explicit calculations of the thermodynamic functions for dense, high-temperature hydrogenic plasmas relevant to inertially-confined-fusion experiments and the interior of the main-sequence stars. The numerical results are parametrized in the form of analytic fitting formulas with a good accuracy.

For the interpretation of the calculated results we paid particular attention to (i) the difference between the two-component plasma system itself and a model system constructed by superposition of the electronic and ionic one-component plasmas, (ii) modification arising from the varied degrees of electron degeneracy, and (iii) the non-RPA, strong-coupling effects described by the LFC's. The importance of including all of these effects has been explicitly demonstrated.

ACKNOWLEDGMENTS

We wish to thank Dr. H. Iyetomi and Dr. K. Utsumi for useful discussions on this and related problems. This work was supported in part through Grants-in-Aid for Scientific Research, No. 56380001 and No. 59380001, provided by the Japanese Ministry of Education, Science, and Culture.

APPENDIX: SOME INTEGRALS INVOLVING THE FERMI FUNCTION

The Fermi integrals $I_\nu(\alpha)$ are defined by

$$I_\nu(\alpha)=\int_0^\infty dz \frac{z^\nu}{\exp(z-\alpha)+1} . \tag{A1}$$

The normalization condition Eq. (9) is expressed as

$$\theta^{3/2} I_{1/2}(\mu_0/k_BT)=\tfrac{2}{3} . \tag{A2}$$

The pressure P_0 of the ideal-gas electron system is given by

$$\frac{P_0V}{Nk_BT}=\theta^{3/2} I_{3/2}(\mu_0/k_BT) . \tag{A3}$$

We express Eq. (7) as

$$\frac{F_1}{Nk_BT}=-\frac{3\Gamma}{4\pi}\left[\frac{9\pi}{4}\right]^{1/3} J(\theta) . \tag{A4}$$

In Table IV we list the computed values of μ_0/k_BT [from (A2)], $I_{3/2}(\mu_0/k_BT)$ in Eq. (A3), and $J(\theta)$ in Eq. (A4).

[1]S. Ichimaru, S. Mitake, S. Tanaka, and X.-Z. Yan, this issue, Phys. Rev. A **32**, 1768 (1985) (paper I).

[2]S. Mitake, S. Tanaka, X.-Z. Yan, and S. Ichimaru, preceding paper, Phys. Rev. A **32**, 1775 (1985) (paper II).

[3]W. B. Hubbard and W. L. Slattery, Astrophys. J. **168**, 131 (1971); H. E. DeWitt and W. B. Hubbard, *ibid.* **205**, 295 (1976).

[4]S. Galam and J. P. Hansen, Phys. Rev. A **14**, 816 (1976).

[5]H. Iyetomi, K. Utsumi, and S. Ichimaru, J. Phys. Soc. Jpn. **50**, 3769 (1981).

[6]J. P. Hansen and I. R. McDonald, Phys. Rev. A **23**, 2041 (1981).

[7]W. Ebeling and W. Richert, Ann. Phys. (Leipzig) **39**, 362 (1982).

[8]U. Gupta and A. K. Rajagopal, Phys. Rev. A **21**, 2064 (1980); **22**, 2792 (1980); Phys. Rep. **87**, 259 (1982).

[9]M. W. C. Dharma-wardana and R. Taylor, J. Phys. C **14**, 629 (1981).

[10]S. Ichimaru, Rev. Mod. Phys. **54**, 1017 (1982).

[11]A. L. Fetter and J. D. Walecka, *Quantum Theory of Many-Particle Systems* (McGraw-Hill, New York, 1971), Chap. 8.

[12]B. Brami, J. P. Hansen, and F. Joly, Physica (Utrecht) **95A**, 505 (1979).

[13]E. M. Lifshitz and L. P. Pitaevskii, *Statistical Physics* (Pergamon, London, 1980), Part 1, p. 94.

[14]M. Baus and J. P. Hansen, Phys. Rep. **59**, 1 (1980).

[15]M. A. Pokrant, Phys. Rev. A **16**, 413 (1977).